Hindawi
Complexity
Volume 2020, Article ID 1874212, 14 pages
https://doi.org/10.1155/2020/1874212

Research Article

A Hybrid Fault-Tolerant Control for Nonlinear Active Suspension Systems Subjected to Actuator Faults and Road Disturbances

Hui Pang, Xue Liu, Yuting Shang, and Rui Yao

School of Mechanical and Precision Instrument Engineering, Xi'an University of Technology, Xi'an 710048, China

Correspondence should be addressed to Hui Pang; huipang@163.com

Received 7 October 2019; Revised 28 November 2019; Accepted 30 December 2019; Published 22 January 2020

Academic Editor: Xianming Zhang

This paper proposes a hybrid fault-tolerant control strategy for nonlinear active suspension subjected to actuator faults and road disturbances. First, an augmented closed-loop system model is established for the nonlinear active suspension system with the actuator faults and road disturbances. Then, based on this model, a hybrid fault-tolerant controller that consists of a nominal state-feedback controller and a robust H_∞ observer is proposed to stabilize the control plant under fault-free condition and further compensate for the suspension performance loss under the actuator fault condition. Finally, a half-vehicle active suspension example is exploited to demonstrate the effectiveness of the proposed hybrid fault-tolerant controller under various running conditions.

1. Introduction

As one of key components in chassis system, vehicle suspension systems connect the vehicle body and wheel to provide a support force and further to improve vehicle dynamics performance [1], and they are usually categorized into three types as passive suspension, semiactive suspension, and active suspension systems [2]. For the passive and semiactive suspension systems, both of them are limited in their ability to possess sufficient ride quality and handling stability [3–5]. While active suspension system (ASS) has the best potentials to make a well trade-off between the conflicting performance requirements [6] and to provide much better ride quality and handling capability [7–9], this is because the actuator assembled in the ASS can generate an extra control force with dissipating the kinetic energy.

Up to now, a number of control algorithms such as H_∞ control [10, 11], sliding-mode control [12], adaptive backstepping control [13, 14], and T-S fuzzy control [15, 16] have been proposed and employed to study vehicle ASSs. However, the existing control schemes in this research field are almost based on such an assumption that all components of vehicle ASSs are under fault-free condition. In fact, it is fairly common to encounter different faults in the real-world suspension system, especially the actuator faults. It should be noticed that the actuator faults would usually result in performance degradation, instability, or catastrophic events for the vehicle suspension system. Consequently, many scholars have devoted their efforts in developing a class of fault-tolerant controller that could deal with the performance loss caused by the actuator faults and then maintain a desirable system performance for the controlled suspension system (see [17–25] and the references therein). Among which, the design of robust H_∞ fault-tolerant control for the ASSs with actuator faults has attracted great attention.

For instance, an H_∞ robust controller was proposed in [26] to guarantee asymptotic stability of the ASSs with three different types of actuator failures. A reliable fuzzy H_∞ robust fault-tolerant controller in [27] was developed for vehicle ASSs with the actuator delay and fault via Takagi-Sugeno (T-S) fuzzy approach. In [28], an adaptive robust fault-tolerant controller was proposed to deal with the problem of fault accommodation for the unknown actuator failures in the ASSs. However, the aforementioned literatures have almost focused on developing a practically passive fault-tolerant controller with preknown fault modes. In

other words, those designed fault-tolerant controllers are not very sensitive to deal with the application scenarios for the ASSs with the single or multimode actuator faults.

To overcome this problem, a fault-tolerant control algorithm was developed in [29] for vehicle ASSs in the finite-frequency domain under the sinusoidal wave fault. In addition, an adaptive fault-tolerant compensation controller was proposed in [30] to enhance the output performance for a kind of vehicle suspension system, wherein the failure model was described by a scalar Markovian type function. A robust H_∞ proportional-integral observer-based fault diagnosis method for the vehicle suspension system was addressed in [31], wherein the constant gain fault was diagnosed by an observer. However, these fault-tolerant control designs did not take the suspension's nonlinearities as well as the actuator faults into account when designing the corresponding controllers; moreover, the fault estimation accuracy has to be considered and enhanced if one wants to develop an effective fault-tolerant controller. Therefore, it is still an interesting and challenging issue to design an appropriate fault-tolerant controller with higher accuracy and better performance for vehicle ASSs.

In the context of the above discussions, this paper proposes a hybrid fault-tolerant control design for nonlinear active suspension subjected to the actuator faults and road disturbances. Herein, compared with the most related fault-tolerant control methods in [16, 19, 21, 31, 32], we make several steps forward. **First**, an augmented closed-loop system model is established for the nonlinear active suspension system with the actuator faults and road disturbances, which were rarely present in the previous papers. **Second**, a hybrid fault-tolerant controller (HFTC) that consists of a nominal state-feedback controller and a robust H_∞ observer is proposed to stabilize the ASS under fault-free condition and compensate for the suspension performance loss under the actuator fault condition. **Third**, a numerical example under various running conditions is presented to reveal the advantages arising from our proposed controller, and some comparative investigations are also provided to validate the control effects of the designed HFTC.

The remainder of this paper is structured as follows. In Section 2, problem formulation is presented. Section 3 provides the robust H_∞ observer design, and Section 4 provides the proposed HFTC synthesis. Section 5 gives the simulation investigation and discussion, and the conclusions are outlined in Section 6.

Notations. $\mathbf{R}^n$ and $\mathbf{R}^{n\times m}$ denote the n-dimensional Euclidean space and the set of $n\times m$ real matrices, respectively. The superscript T is used to represent the transposition of the matrix. And for the symmetric matrices $\mathbf{X}$ and $\mathbf{Y}$, $\mathbf{X}-\mathbf{Y}$ is positive semidefinite for $\mathbf{X}\geq\mathbf{Y}$ and positive definite for $\mathbf{X}>\mathbf{Y}$, respectively. L^2 stands for the space of square-integral vector functions. $\|\cdot\|$ stands for the Euclidean vector norm, and the asterisk $(*)$ denotes the symmetric form of a matrix. The space of square-integral vector functions over $[0, +\infty)$ is denoted by $L_2\,[0, +\infty)$, and for $w=\in L_2\,[0, +\infty)$, its norm is given by $\|w\| = \sqrt{\int_{t=0}^{\infty}|w|^2\mathrm{d}t}$. T_{zw} denotes the transfer function of the closed-loop system from the road disturbance w to the control output z.

2. Problem Formulation

In this section, a control-oriented half-vehicle active suspension model with four degrees of freedom (4-DOFs) shown in Figure 1 is used to develop our fault-tolerant controller.

Based on Newton's second law, we can easily construct the dynamics equations of this half-vehicle ASS as

$$\begin{cases} \mathbf{M}_s\ddot{\mathbf{q}} = \mathbf{G}\mathbf{K}_s\left(\mathbf{z}_u-\mathbf{z}_s\right)+\mathbf{G}\mathbf{C}_s\left(\dot{\mathbf{z}}_u-\dot{\mathbf{z}}_s\right)-\mathbf{G}\mathbf{v}_1\left(\mathbf{z}_u-\mathbf{z}_s\right) \\ \quad -\mathbf{G}\mathbf{v}_2\left(\dot{\mathbf{z}}_u-\dot{\mathbf{z}}_s\right)+\mathbf{G}\mathbf{u}, \\ \mathbf{M}_u\ddot{\mathbf{z}}_u = \mathbf{K}_s\left(\mathbf{z}_s-\mathbf{z}_u\right)+\mathbf{C}_s\left(\dot{\mathbf{z}}_s-\dot{\mathbf{z}}_u\right)+\mathbf{K}_u\left(\mathbf{z}_r-\mathbf{z}_u\right) \\ \quad +\mathbf{v}_1\left(\mathbf{z}_u-\mathbf{z}_s\right)+\mathbf{v}_2\left(\dot{\mathbf{z}}_u-\dot{\mathbf{z}}_s\right)-\mathbf{u}, \end{cases} \tag{1}$$

where $\mathbf{q}=[z_c,\ \phi]^T$ is the output performance vector, $\mathbf{z}_s=[z_{sf},\ z_{sr}]^T$ is the sprung-mass displacement vector, $\mathbf{z}_u=[z_{uf},\ z_{ur}]^T$ is the suspension displacement vector, $\mathbf{z}_r=[z_{rf},\ z_{rr}]^T$ is the input vector of the road disturbances at the front and rear wheel, $\mathbf{u}=[u_{tf},\ u_{tr}]^T$ is the desirable control forces, and $\mathbf{v}_1\left(\mathbf{z}_s-\mathbf{z}_u\right)$ and $\mathbf{v}_2\ (\dot{z}_s-\dot{z}_u)$ are the nonlinear term originated from the nonlinear characteristics of vehicle suspension damper and spring, respectively.

In equation (1), the corresponding coefficient matrices are given by

$$\begin{aligned} \mathbf{M}_s &= \begin{bmatrix} m_s & 0 \\ 0 & I_y \end{bmatrix}, \\ \mathbf{M}_u &= \begin{bmatrix} m_{uf} & 0 \\ 0 & m_{ur} \end{bmatrix}, \\ \mathbf{C}_s &= \begin{bmatrix} c_f & 0 \\ 0 & c_r \end{bmatrix}, \\ \mathbf{K}_s &= \begin{bmatrix} k_f & 0 \\ 0 & k_r \end{bmatrix}, \\ \mathbf{K}_u &= \begin{bmatrix} k_{tf} & 0 \\ 0 & k_{tr} \end{bmatrix}, \\ \mathbf{G} &= \begin{bmatrix} 1 & 1 \\ -a & b \end{bmatrix}. \end{aligned} \tag{2}$$

Define $\mathbf{x}=[\mathbf{z}_s-\mathbf{z}_u,\ \dot{z}_s,\ \mathbf{z}_u-\mathbf{z}_r,\ \dot{z}_u]^T$ as the system state vector and let $\mathbf{w}=\mathbf{z}_r$, $\mathbf{y}=[\mathbf{z}_u-\mathbf{z}_r,\ \dot{z}_s]^T$ as the measured output vector and $\mathbf{z}=[\ddot{q},\ \mathbf{z}_s-\mathbf{z}_u,\ \mathbf{K}_u\ (\mathbf{z}_u-\mathbf{z}_r),\ \mathbf{u}]^T$ as the system output vector. Then, the state-space form of the ASS without the actuator faults is written as

$$\begin{cases} \dot{\mathbf{x}} = \mathbf{A}\mathbf{x}+\mathbf{B}_1\mathbf{w}+\mathbf{B}_2\mathbf{u}+\mathbf{D}_1\mathbf{v}, \\ \mathbf{y} = \mathbf{C}_1\mathbf{x}, \\ \mathbf{z} = \mathbf{C}_2\mathbf{x}+\mathbf{D}_2\mathbf{u}, \end{cases} \tag{3}$$

wherein the corresponding coefficients matrices are described as follows:

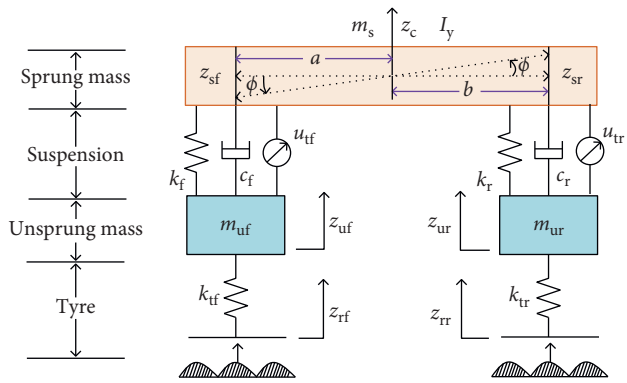

FIGURE 1: Half-vehicle active suspension model.

$$\mathbf{A} = \begin{bmatrix} \mathbf{0} & \mathbf{I} & \mathbf{0} & -\mathbf{I} \\ -\mathbf{G}^T\mathbf{M}_s^{-1}\mathbf{G}\mathbf{K}_s & -\mathbf{G}^T\mathbf{M}_s^{-1}\mathbf{G}\mathbf{C}_s & \mathbf{0}_{2\times 2} & \mathbf{G}^T\mathbf{M}_s^{-1}\mathbf{G}\mathbf{C}_s \\ \mathbf{0} & \mathbf{0} & \mathbf{0} & \mathbf{I} \\ \mathbf{M}_u^{-1}\mathbf{K}_s & \mathbf{M}_u^{-1}\mathbf{C}_s & -\mathbf{M}_u^{-1}\mathbf{K}_u & -\mathbf{M}_u^{-1}\mathbf{C}_s \end{bmatrix},$$

$$\mathbf{B}_1 = \begin{bmatrix} \mathbf{0} \\ \mathbf{0} \\ -\mathbf{I} \\ \mathbf{0} \end{bmatrix},$$

$$\mathbf{B}_2 = \begin{bmatrix} \mathbf{0} \\ \mathbf{G}^T\mathbf{M}_s^{-1}\mathbf{G} \\ \mathbf{0} \\ \mathbf{M}_u^{-1} \end{bmatrix},$$

$$\mathbf{C}_1 = \begin{bmatrix} \mathbf{I} & \mathbf{0} \end{bmatrix},$$

$$\mathbf{C}_2 = \begin{bmatrix} -\mathbf{M}_s^{-1}\mathbf{G}\mathbf{K}_s & -\mathbf{M}_s^{-1}\mathbf{G}\mathbf{C}_s & \mathbf{0} & \mathbf{M}_s^{-1}\mathbf{G}\mathbf{C}_s \\ \mathbf{I} & \mathbf{0} & \mathbf{0} & \mathbf{0} \\ \mathbf{0} & \mathbf{0} & \mathbf{K}_u & \mathbf{0} \\ \mathbf{0} & \mathbf{0} & \mathbf{0} & \mathbf{0} \end{bmatrix},$$

$$\mathbf{D}_1 = \begin{bmatrix} \mathbf{G}^T\mathbf{M}_s^{-1}\mathbf{G} & \mathbf{0} & \mathbf{0} & \mathbf{0} \\ \mathbf{0} & \mathbf{M}_u^{-1} & \mathbf{0} & \mathbf{0} \\ \mathbf{0} & \mathbf{0} & \mathbf{0} & \mathbf{0} \\ \mathbf{0} & \mathbf{0} & \mathbf{0} & \mathbf{M}_u^{-1} \end{bmatrix},$$

$$\mathbf{D}_2 = \begin{bmatrix} -\mathbf{M}_s^{-1}\mathbf{G} & \mathbf{0} & \mathbf{0} & \mathbf{0} \end{bmatrix}. \tag{4}$$

It should be noticed that $\mathbf{v}(\mathbf{x}, t) = [\mathbf{v}_1(\mathbf{z}_s - \mathbf{z}_u), \mathbf{v}_2(\dot{z}_s - \dot{z}_u)]^T$ is the nonlinear term vector, $\mathbf{I}$ is an identity matrix with appropriate dimension, and the dependent variables of $\mathbf{x}$ and t in $\mathbf{v}(\mathbf{x},t)$ are usually omitted for brevity. Besides, to facilitate the description of the suspension system, the following two assumptions are given.

Assumption 1. In this work, it is assumed that the nonlinear terms $\mathbf{v}_1$ and $\mathbf{v}_2$ satisfy the Lipschitz condition as follows [33]:

$$\begin{aligned} \left\|\mathbf{v}_1(\mathbf{z}_s - \mathbf{z}_u)\right\| &\le \left\|V_k\mathbf{K}_s(\mathbf{z}_s - \mathbf{z}_u)\right\|, \\ \left\|\mathbf{v}_2(\dot{\mathbf{z}}_s - \dot{\mathbf{z}}_u)\right\| &\le \left\|V_c\mathbf{C}_s(\dot{\mathbf{z}}_s - \dot{\mathbf{z}}_u)\right\|, \end{aligned} \tag{5}$$

where V_k and V_c are the quantized factor that represent for the nonlinear perturbations of the spring and damper coefficients, respectively, and the values of V_c and V_k are selected as $V_c = V_k = 0.1$.

Assumption 2. It is assumed that the actuator fault f along with its corresponding derivatives $\dot{\mathbf{f}}$ satisfies $\mathbf{f} \in L_2[0\,\infty)$, and $\dot{\mathbf{f}} \in L_2[0\,\infty)$.

Remark 1. It is assumed that the energy of actuator fault is bounded with satisfying $\mathbf{f} \in L_2[0\,\infty)$, and it is accordingly inferred that the derivatives of actuator fault are satisfied with $\dot{\mathbf{f}} \in L_2[0\,\infty)$.

With the above two assumptions, the state-space equations of this faulty ASS can be derived as

$$\begin{cases} \dot{\mathbf{x}}_f = \mathbf{A}\mathbf{x}_f + \mathbf{B}_1\mathbf{w} + \mathbf{B}_f\mathbf{f} + \mathbf{B}_2\mathbf{u}_f + \mathbf{D}_1\mathbf{v}, \\ \mathbf{y}_f = \mathbf{C}_1\mathbf{x}_f + \mathbf{D}_{1f}\mathbf{f}, \\ \mathbf{z}_f = \mathbf{C}_2\mathbf{x}_f + \mathbf{D}_2\mathbf{u}_f + \mathbf{D}_{2f}\mathbf{f}, \end{cases} \tag{6}$$

where $\mathbf{f} \in \mathbf{R}^n$ is the actuator fault vector and $\mathbf{B}_f$, $\mathbf{D}_{1f}$, and $\mathbf{D}_{2f}$ are the coefficient matrices with appropriate dimension, satisfying $\begin{bmatrix} \mathbf{B}_f^T & \mathbf{D}_{2f}^T \end{bmatrix}^T = \begin{bmatrix} \mathbf{B}_2^T & \mathbf{D}_2^T \end{bmatrix}^T \cdot \mathbf{M}$.

Remark 2. $\begin{bmatrix} \mathbf{B}_f^T & \mathbf{D}_{2f}^T \end{bmatrix}^T = \begin{bmatrix} \mathbf{B}_2^T & \mathbf{D}_2^T \end{bmatrix}^T \cdot \mathbf{M}$ means that the actuator faults usually occur in the same channel of a fault-tolerant controller, implying the match of the actuator faults. If the actuator faults are matched, then the negative effects caused by the faults can be compensated by the designed fault-tolerant controller. This condition may be a constraint on the hybrid fault-tolerant control method, but it is very practical and common in the fault-tolerant control community.

Furthermore, the actuator fault vector f considered herein is subjected to an exogenous system [34, 35]. Without loss of generality, the generalized fault signal model can be described as

$$\begin{cases} \dot{\mathbf{x}}_{ef} = \mathbf{A}_{wf}\mathbf{x}_{ef} + \mathbf{B}_{wf}\boldsymbol{\delta}, \\ \mathbf{f} = \mathbf{C}_{wf}\mathbf{x}_{ef}, \end{cases} \tag{7}$$

where $\mathbf{x}_{ef} \in R^{n_f}$ denotes the state vector of the exogenous system, $\boldsymbol{\delta}$ denotes a bounded virtual input signal, and $\mathbf{A}_{wf}$, $\mathbf{B}_{wf}$, and $\mathbf{C}_{wf}$ denote the coefficient matrices with appropriate dimension.

Remark 3. Failures can be manifested in the breakdown of a piece of equipment (hard failure, e.g., partial blockage or stuck) or gradual degradation (incipient or soft failures, e.g., natural wear and tear and system degradation) in the active suspension system. There may be various kinds of actuator faults, but they can be theoretically modeled in a finite parameter family named as slow drift fault, constant gain fault or sinusoidal fault, and so on for the control strategy design process.

Besides, in this work, the main reasons of employing this fault expression as shown in (7) lie in the following two aspects. (1) An explicit fault diagnosis module is not needed in the proposed fault-tolerant controller synthesis. (2) This actuator fault signal model is helpful for the subsequent system augmentation since it would be intrinsically embedded in the controller design.

By combing (7) with (6) with the aforementioned assumptions and system augmentation technique, we can obtain

$$\begin{cases} \dot{\overline{\mathbf{x}}} = \mathbf{A}_{\mathrm{ef}}\overline{\mathbf{x}} + \mathbf{B}_{\mathrm{ef}}\mathbf{u} + \mathbf{F}_{\mathrm{e}}\widetilde{w} + \mathbf{F}, \\ \mathbf{y} = \mathbf{C}_{\mathrm{e}}\overline{\mathbf{x}}, \\ \mathbf{f} = \mathbf{C}_{\mathrm{ef}}\overline{\mathbf{x}}, \end{cases} \tag{8}$$

where

$$\begin{aligned} \overline{\mathbf{x}} &= \begin{bmatrix} \mathbf{x}_{\mathrm{f}} \\ \mathbf{x}_{\mathrm{ef}} \end{bmatrix}, \\ \widetilde{\mathbf{w}} &= \begin{bmatrix} \mathbf{w} \\ \boldsymbol{\delta} \end{bmatrix}, \\ \mathbf{A}_{\mathrm{ef}} &= \begin{bmatrix} \mathbf{A} & \mathbf{B}_{\mathrm{f}}\mathbf{C}_{\mathrm{wf}} \\ \mathbf{0} & \mathbf{A}_{\mathrm{wf}} \end{bmatrix}, \\ \mathbf{B}_{\mathrm{ef}} &= \begin{bmatrix} \mathbf{B}_2 \\ \mathbf{0} \end{bmatrix}, \\ \mathbf{F}_{\mathrm{e}} &= \begin{bmatrix} \mathbf{F}_{1\mathrm{e}} & \mathbf{F}_{2\mathrm{e}} \end{bmatrix}, \\ \mathbf{F}_{1\mathrm{e}} &= \begin{bmatrix} \mathbf{B}_1 \\ \mathbf{0} \end{bmatrix}, \\ \mathbf{F}_{2\mathrm{e}} &= \begin{bmatrix} \mathbf{0} \\ \mathbf{B}_{\mathrm{wf}} \end{bmatrix}, \\ \mathbf{F} &= \begin{bmatrix} \mathbf{F}_1\mathbf{v} \\ \mathbf{0} \end{bmatrix}, \\ \mathbf{C}_{\mathrm{ef}} &= \begin{bmatrix} \mathbf{0} & \mathbf{C}_{\mathrm{wf}} \end{bmatrix}, \\ \mathbf{C}_{\mathrm{e}} &= \begin{bmatrix} \mathbf{C}_1 & \mathbf{D}_{1\mathrm{f}}\mathbf{C}_{\mathrm{wf}} \end{bmatrix}. \end{aligned} \tag{9}$$

3. Robust H_∞ Observer Design

This section contributes to establishing a robust H_∞ observer to estimate the unmeasurable actuator faults and the related system states. Before proceeding, it is assumed that the pair $(A_{\mathrm{ef}}, C_{\mathrm{e}})$ in (8) is observable.

Accordingly, an augmented observer is constructed to accurately estimate both of the system states and the fault signals for the ASS, and the full-order observer of system (8) is expressed by

$$\begin{cases} \dot{\widehat{\overline{\mathbf{x}}}} = \mathbf{A}_{\mathrm{ef}}\widehat{\overline{\mathbf{x}}} + \mathbf{B}_{\mathrm{ef}}\mathbf{u}_f + \mathbf{L}\left(\mathbf{y} - \mathbf{C}_{\mathrm{e}}\widehat{\overline{\mathbf{x}}}\right) + \mathbf{F}, \\ \widehat{\mathbf{f}} = \mathbf{C}_{\mathrm{ef}}\widehat{\overline{\mathbf{x}}}, \end{cases} \tag{10}$$

where $\widehat{\overline{\mathbf{x}}} \in R^{n+n_f}$ is estimated state vector and L is the undetermined gain matrix for the augmented observer, respectively.

Let

$$\mathbf{e} = \overline{\mathbf{x}} - \widehat{\overline{\mathbf{x}}}, \tag{11}$$

$$\widetilde{\mathbf{f}} = \mathbf{f} - \widehat{\mathbf{f}}. \tag{12}$$

Differentiating (11) yields

$$\dot{\mathbf{e}} = \dot{\overline{\mathbf{x}}} - \dot{\widehat{\overline{\mathbf{x}}}}. \tag{13}$$

From (12) and (13), we can derive the error system as

$$\begin{cases} \dot{\mathbf{e}} = \left(\mathbf{A}_{\mathrm{ef}} - \mathbf{L}\mathbf{C}_{\mathrm{e}}\right)\mathbf{e} + \mathbf{F}_{\mathrm{e}}\widetilde{w} + \Delta\mathbf{F}, \\ \widetilde{\mathbf{f}} = \mathbf{C}_{\mathrm{ef}}\mathbf{e}, \end{cases} \tag{14}$$

where

$$\Delta\mathbf{F} = \begin{bmatrix} \mathbf{F}_1\mathbf{v}(\mathbf{x}, t) - \mathbf{F}_1\mathbf{v}(\widehat{\mathbf{x}}, t) \\ \mathbf{0} \end{bmatrix}. \tag{15}$$

Then, with the following Definition 1, Theorem 1, and Theorem 2, the existing conditions of the designed robust H_∞ observer can be obtained so as to ensure the H_∞ performances of the closed-loop system under zero initial condition.

Definition 1. For a given $\beta > 0$, the system is said to be of H_∞ performance β if the system is internally asymptotically stable and the inequality $\|\widetilde{\mathbf{f}}\| < \boldsymbol{\beta}\|\widetilde{\mathbf{w}}\|$ holds for $\forall\widetilde{\mathbf{w}} \in L_2[0, +\infty)$ under zero initial conditions.

Theorem 1. *For given positive scalars α and β, the closed-loop system (13) is asymptotically stable and has a prescribed H_∞ disturbance attenuation level $\beta > 0$, if there exist symmetric positive definite matrix P_1 with appropriate dimension and a gain matrix L such that the following inequality holds:*

$$\begin{bmatrix} \left(\mathbf{A}_{\mathrm{ef}} - \mathbf{L}\mathbf{C}_{\mathrm{e}}\right)^T\mathbf{P}_1 + \mathbf{P}_1\left(\mathbf{A}_{\mathrm{ef}} - \mathbf{L}\mathbf{C}_{\mathrm{e}}\right) + \mathbf{C}_{\mathrm{ef}}^T\mathbf{C}_{\mathrm{ef}} & \mathbf{P}_1 & \mathbf{P}_1\mathbf{F}_{\mathrm{e}} \\ * & -\mathbf{I} & \mathbf{0} \\ * & * & -\beta\mathbf{I} \end{bmatrix} < 0. \tag{16}$$

Proof. Define the Lyapunov function as

$$\mathbf{V}_1 = \mathbf{e}^T\mathbf{P}_1\mathbf{e}. \tag{17}$$

The time derivative of (17) becomes

$$\begin{aligned} \dot{\mathbf{V}}_1 = \dot{\mathbf{e}}^T\mathbf{P}_1\mathbf{e} + \mathbf{e}^T\mathbf{P}_1\dot{\mathbf{e}} = \mathbf{e}^T\Big(&\left(\mathbf{A}_{\mathrm{ef}} - \mathbf{L}\mathbf{C}_{\mathrm{e}}\right)^T\mathbf{P}_1 \\ &+ \mathbf{P}_1\left(\mathbf{A}_{\mathrm{ef}} - \mathbf{L}\mathbf{C}_{\mathrm{e}}\right)\Big)\mathbf{e} + 2\mathbf{e}^T\mathbf{P}_1\mathbf{F}_{\mathrm{e}}\widetilde{\mathbf{w}} + 2\mathbf{e}^T\mathbf{P}_1\Delta\mathbf{F}. \end{aligned} \tag{18}$$

It can be derived from Lipschitz condition [33] that

$$\|\Delta\mathbf{F}\|^2 = \|\mathbf{F}(\mathbf{x}, t) - \mathbf{F}(\widehat{\mathbf{x}}, t)\|^2 \le \alpha^2\|\mathbf{e}\|^2. \tag{19}$$

That is,

$$\Delta\mathbf{F}^T\Delta\mathbf{F} - \alpha^2\mathbf{e}^T\mathbf{e} \le 0. \tag{20}$$

From (18) and (20), we have

$$\dot{\mathbf{V}}_1 \le \mathbf{e}^T\Big(\left(\mathbf{A}_{\mathrm{ef}} - \mathbf{L}\mathbf{C}_{\mathrm{e}}\right)^T\mathbf{P}_1 + \mathbf{P}_1\left(\mathbf{A}_{\mathrm{ef}} - \mathbf{L}\mathbf{C}_{\mathrm{e}}\right)\Big)\mathbf{e} + 2\mathbf{e}^T\mathbf{P}_1\mathbf{F}_{\mathrm{e}}\tilde{\mathbf{w}} + 2\mathbf{e}^T\mathbf{P}_1\Delta\mathbf{F} + \alpha^2\mathbf{e}^T\mathbf{e} - \Delta\mathbf{F}^T\Delta\mathbf{F}. \tag{21}$$

Let the external road disturbance $\tilde{\mathbf{w}} = 0$, and in terms of (21), we obtain

$$\dot{\mathbf{V}}_1 \le \mathbf{g}_1^T\psi_1\mathbf{g}_1, \tag{22}$$

where

$$\mathbf{g}_1 = \begin{bmatrix} \mathbf{e} \\ \Delta\mathbf{F} \end{bmatrix}, \quad \psi_1 = \begin{bmatrix} \left(\mathbf{A}_{\mathrm{ef}} - \mathbf{L}\mathbf{C}_{\mathrm{e}}\right)^T\mathbf{P}_1 + \mathbf{P}_1\left(\mathbf{A}_{\mathrm{ef}} - \mathbf{L}\mathbf{C}_{\mathrm{e}}\right) + \alpha^2\mathbf{I} & \mathbf{P}_1 \\ * & -\mathbf{I} \end{bmatrix}. \tag{23}$$

It can be inferred from (22) that if $\psi_1 < 0$, one gets $\dot{\mathbf{V}} < 0$, and system (13) is asymptotically stable with $\tilde{\mathbf{w}} = 0$.

Next, consider the H_∞ performance index β with $\forall\tilde{w} \in L_2[0, +\infty)$; if we assume $\mathbf{V}_1|_{t=0} = 0$, then the performance index $\mathbf{J}_{\mathrm{w}}$ can be defined as

$$\mathbf{J}_{\mathrm{w}} = \int_0^\infty \left(\tilde{\mathbf{f}}^T\tilde{\mathbf{f}} - \beta\tilde{w}^T\right)\tilde{\mathbf{w}}\,\mathrm{d}t. \tag{24}$$

Because $\mathbf{V}|_{t=0} = 0$ and $\mathbf{V}_1(\infty) \ge 0$, in terms of (21) and (24), we can obtain

$$\begin{aligned} \mathbf{J}_{\mathrm{w}} &= \int_0^\infty \left(\tilde{\mathbf{f}}^T\tilde{\mathbf{f}} - \beta\tilde{\mathbf{w}}^T\tilde{\mathbf{w}}\right) + \dot{\mathbf{V}}\mathrm{d}t - \mathbf{V}_1(\infty) + \mathbf{V}_1(0) \\ &\le \int_0^\infty \left(\tilde{\mathbf{f}}^T\tilde{\mathbf{f}} - \beta\tilde{\mathbf{w}}^T\tilde{\mathbf{w}} + \dot{\mathbf{V}}_1\right)\mathrm{d}t \\ &\le \int_0^\infty \mathbf{e}^T\Big(\left(\mathbf{A}_{\mathrm{ef}} - \mathbf{L}\mathbf{C}_{\mathrm{e}}\right)^T\mathbf{P} + \mathbf{P}_1\left(\mathbf{A}_{\mathrm{ef}} - \mathbf{L}\mathbf{C}_{\mathrm{e}}\right)\Big)\mathbf{e} \\ &\quad + 2\mathbf{e}^T\mathbf{P}_1\mathbf{F}_{\mathrm{e}}\tilde{\mathbf{w}} + 2\mathbf{e}^T\mathbf{P}_1\Delta\mathbf{F}(\mathbf{x}, t) + \alpha^2\mathbf{e}^T\mathbf{e} \\ &\quad - \Delta\mathbf{F}(\mathbf{x}, t)^T\Delta\mathbf{F}(\mathbf{x}, t) + \mathbf{e}^T\left(\mathbf{C}_{\mathrm{ef}}^T\mathbf{C}_{\mathrm{ef}}\mathbf{e} - \beta\tilde{\mathbf{w}}^T\tilde{\mathbf{w}}\right)\mathrm{d}t. \end{aligned} \tag{25}$$

Let

$$\zeta_1 = \begin{bmatrix} e \\ \Delta\mathbf{F}(\mathbf{x}, t) \\ \tilde{\mathbf{w}} \end{bmatrix}, \quad \psi_2 = \begin{bmatrix} \left(\mathbf{A}_{\mathrm{ef}} - \mathbf{L}\mathbf{C}_{\mathrm{e}}\right)^T\mathbf{P}_1 + \mathbf{P}_1\left(\mathbf{A}_{\mathrm{ef}} - \mathbf{L}\mathbf{C}_{\mathrm{e}}\right) + \mathbf{C}_{\mathrm{ef}}^T\mathbf{C}_{\mathrm{ef}} + \alpha^2\mathbf{I} & \mathbf{P}_1 & \mathbf{P}_1\mathbf{F}_{\mathrm{e}} \\ * & -\mathbf{I} & 0 \\ * & * & -\beta\mathbf{I} \end{bmatrix}. \tag{26}$$

If $\psi_2 < 0$, then we can get

$$\mathbf{J}_{\mathrm{w}} = \int_0^\infty \left(\tilde{\mathbf{f}}^T\tilde{\mathbf{f}} - \beta\tilde{w}^T\tilde{w}\right)\mathrm{d}t \le \int_0^\infty \zeta_1^T\psi_2\zeta_1\,\mathrm{d}t < 0. \tag{27}$$

It is equivalent to

$$\|\tilde{\mathbf{f}}\| < \beta\|\tilde{\mathbf{w}}\|. \tag{28}$$

By using Schur complement [36], one can get $\psi_1 < 0$ with $\psi_2 < 0$, and the condition of $\psi_2 < 0$ guarantees $\dot{\mathbf{V}}_1 < 0$; thus, system (13) is asymptotically stable. For $\forall\mathbf{w} \in L_2[0, +\infty)$, we obtain $\mathbf{J}_{\mathrm{w}} < 0$ in terms of $\dot{\mathbf{V}}_1 < 0$, i.e., $\|\tilde{\mathbf{f}}\| < \beta\|\tilde{\mathbf{w}}\|$. Furthermore, system (13) has H_∞ performance β when it is asymptotically stable and the inequality $\|\tilde{\mathbf{f}}\| < \beta\|\tilde{\mathbf{w}}\|$ holds for $\forall\mathbf{w} \in L_2[0, +\infty)$ under $\psi_2 < 0$ conditions. The proof is completed.

Since *Theorem 1* involves the expression like $\mathbf{P}_1\mathbf{L}\mathbf{C}_{\mathrm{e}}$, it cannot be solved directly via the LMI technique, and then *Theorem 2* is introduced in the following form to cope with this problem. □

Theorem 2. *For given positive scalars α and β, the closed-loop system (13) is asymptotically stable and has a prescribed H_∞ disturbance attenuation level $\beta > 0$, if there exist symmetric positive matrices P_1, Y_1 with appropriate dimension and the gain matrix* **L** *such that the following inequality holds:*

$$\begin{bmatrix} \mathbf{A}_{\mathrm{ef}}^T\mathbf{P}_1 + \mathbf{P}_1\mathbf{A}_{\mathrm{ef}} - \mathbf{C}_{\mathrm{e}}^T\mathbf{Y}_1^T - \mathbf{Y}_1\mathbf{C}_{\mathrm{e}} + \mathbf{C}_{\mathrm{ef}}^T\mathbf{C}_{\mathrm{ef}} + \alpha^2\mathbf{I} & \mathbf{P}_1 & \mathbf{P}_1\mathbf{F}_{\mathrm{e}} \\ * & -\mathbf{I} & \mathbf{0} \\ * & * & -\beta\mathbf{I} \end{bmatrix} < 0, \tag{29}$$

where $\mathbf{L} = \mathbf{P}_1^{-1}\mathbf{Y}$.

Proof. Substituting Y_1=P_1L into (16), one can obtain (29).

The proof is completed.

Obviously, with *Theorem 2*, system (13) has H_∞ performance β when the system is asymptotically stable and the inequality $\|\tilde{\mathbf{f}}\| < \beta\|\tilde{\mathbf{w}}\|$; thus, we get $\hat{\mathbf{f}} \cong \mathbf{f}$ from the full-order observer in (10). Next, the proposed fault-tolerant controller synthesis will be discussed in Section 4. □

4. Hybrid Fault-Tolerant Controller Synthesis

4.1. Design of H_∞ Observer-Based Fault-Tolerant Controller. To begin with, the fault-tolerant controller involved with $\mathbf{x}_{\mathrm{f}}$ and $\hat{\mathbf{f}}$ is designed as

$$\mathbf{u}_{\mathrm{f}} = \mathbf{u}_{\mathrm{n}} + \mathbf{u}_{\mathrm{c}}, \tag{30}$$

where $\mathbf{u}_{\mathrm{f}}$ is the desirable control force of the proposed fault-tolerant controller, $\mathbf{u}_{\mathrm{n}} = \mathbf{K}\mathbf{x}_{\mathrm{f}}$ is nominal state-feedback controller, $\mathbf{u}_{\mathrm{c}} = -\mathbf{M}\hat{\mathbf{f}}$ is H_∞ observer-based compensation controller, $\mathbf{K}$ is the gain matrix of nominal state-feedback controller, $\hat{\mathbf{f}}$ is the actuator fault estimation achieved by the designed robust H_∞ observer in (10), and $\mathbf{M}$ is a known matrix with appropriate dimension.

Substituting (30) into (6) results in (31) as

$$\begin{cases} \dot{\mathbf{x}}_{\mathrm{f}} = \overline{\mathbf{A}}\mathbf{x}_{\mathrm{f}} + \mathbf{B}_1\mathbf{w} + \mathbf{F}_1\mathbf{v}, \\ \mathbf{z}_{\mathrm{f}} = \overline{\mathbf{C}}_2\mathbf{x}_{\mathrm{f}}, \end{cases} \tag{31}$$

where $\overline{\mathbf{A}} = \mathbf{A} + \mathbf{B}_2\mathbf{K}$ and $\overline{\mathbf{C}}_2 = \mathbf{C}_2 + \mathbf{D}_2\mathbf{K}$.

Additionally, according to (5), we can obtain

$$\|\mathbf{v}\| \le \left\| \begin{bmatrix} \mathbf{V}_{\mathrm{k}}K_{\mathrm{s}} & 0 & 0 & 0 \\ 0 & \mathbf{V}_{\mathrm{c}}\mathbf{C}_{\mathrm{s}} & 0 & 0 \\ 0 & 0 & 0 & 0 \\ 0 & 0 & 0 & -\mathbf{V}_{\mathrm{c}}\mathbf{C}_{\mathrm{s}} \end{bmatrix} \begin{bmatrix} \left(\mathbf{z}_{\mathrm{s}} - \mathbf{z}_{\mathrm{u}}\right) \\ \dot{\mathbf{z}}_{\mathrm{s}} \\ \left(\mathbf{z}_{\mathrm{u}} - \mathbf{z}_{\mathrm{r}}\right) \\ \dot{\mathbf{z}}_{\mathrm{u}} \end{bmatrix} \right\| = \left\|\mathbf{W}_1\mathbf{x}\right\|, \tag{32}$$

where

$$\mathbf{W}_1 = \begin{bmatrix} \mathbf{V}_k K_s & 0 & 0 & 0 \\ 0 & \mathbf{V}_c C_s & 0 & 0 \\ 0 & 0 & 0 & 0 \\ 0 & 0 & 0 & -\mathbf{V}_c C_s \end{bmatrix}. \tag{33}$$

Thus far, the proposed H_∞ state-feedback controller can be summarized as *Theorem 3* and *Theorem* 4.

Theorem 3. *Given positive scalars γ and λ_2, the closed-loop system (31) is asymptotically stable and has a prescribed H_∞ disturbance attenuation level $\gamma > 0$, if there exists symmetric positive matrix P_2 with appropriate dimension such that the following inequality holds:*

$$\begin{bmatrix} \mathbf{P}_2\overline{\mathbf{A}} + \overline{\mathbf{A}}^T\mathbf{P}_2 + \lambda_2\mathbf{W}_1^T\mathbf{W}_1 + \overline{\mathbf{C}}_2^T\overline{\mathbf{C}}_2 & \mathbf{P}_2\mathbf{F}_1 & \mathbf{P}_2\mathbf{B}_1 \\ * & -\lambda_2\mathbf{I} & 0 \\ * & * & -\gamma\mathbf{I} \end{bmatrix} < 0. \tag{34}$$

Proof. Define the Lyapunov function as

$$V_2 = xP_2x + \left(\int_0^t \lambda_2 \left\| W_1 x \right\|^2 - \lambda_2 \| v(x,t) \|^2 \right) \mathrm{d}t. \tag{35}$$

Let $w = 0$, and taking the derivative of V gives

$$\begin{aligned} \dot{V}_2 &= x^T P_2 \left(\overline{A}x + F_1 v \right) + \left(x^T \overline{A}^T + v^T F_1^T \right) P_2 x \\ &\quad + \lambda_2 \left\| W_1 x \right\|^2 - \lambda_2 \| v \|^2, \\ &= x^T \left(P_2\overline{A} + \overline{A}^T P_2 + \lambda_2 W_1^T W_1 \right) x + x^T P_2 F_1 v \\ &\quad + v^T F_1^T P_2 x - \lambda_2 v^T v, \\ &= \mathbf{g}_2^T \chi \mathbf{g}_2, \end{aligned} \tag{36}$$

where

$$\begin{aligned} \mathbf{g}_2 &= \begin{bmatrix} \mathbf{x} \\ \mathbf{v} \end{bmatrix}, \\ \chi_1 &= \begin{bmatrix} P_2\overline{A} + \overline{A}^T P_2 + \lambda_2 W_1^T W_1 & P_2 F_1 \\ * & \lambda_2 I \end{bmatrix}. \end{aligned} \tag{37}$$

Thus, if $\chi_1 < 0$, then $\dot{\mathbf{V}} < 0$, and the closed-loop system (31) is definitely asymptotically stable. Moreover, consider the H_∞ performance index γ with $\forall \mathbf{w} \in L_2[0, +\infty)$ and suppose $\mathbf{V}_2|_{t=0} = 0$, if we define the performance index $\mathbf{J}_z$ as

$$\mathbf{J}_z = \int_0^\infty \left(\mathbf{z}^T\mathbf{z} - \gamma \mathbf{w}^T\mathbf{w} \right) \mathrm{d}t. \tag{38}$$

Because $\mathbf{V}_2|_{t=0} = 0$ and $\mathbf{V}_2(\infty) \geq 0$, from (36) and (38), we can further get

$$\begin{aligned} \mathbf{J}_z &= \int_0^\infty \left(\mathbf{z}^T\mathbf{z} - \gamma\mathbf{w}^T\mathbf{w} \right) + \dot{\mathbf{V}}\mathrm{d}t - \mathbf{V}_2(\infty) + \mathbf{V}_2(0) \\ &\leq \int_0^\infty \left(\mathbf{z}^T\mathbf{z} - \gamma\mathbf{w}^T\mathbf{w} \right) + \dot{\mathbf{V}}_2 \mathrm{d}t \\ &\leq \int_0^\infty -\gamma\mathbf{w}^T\mathbf{w} + \mathbf{x}^T \left(\mathbf{P}_2\overline{\mathbf{A}} + \overline{\mathbf{A}}^T\mathbf{P}_2 + \lambda_2\mathbf{W}_1^T\mathbf{W}_1 + \overline{\mathbf{C}}_2^T\overline{\mathbf{C}}_2 \right) \mathbf{x} \\ &\quad + \mathbf{x}^T\mathbf{P}_2\mathbf{F}_1\mathbf{v}(\mathbf{x},t) + \mathbf{v}^T\mathbf{F}_1^T\mathbf{P}_2\mathbf{x} + \mathbf{w}^T\mathbf{P}_2\mathbf{B}_1\mathbf{x} \\ &\quad + \mathbf{x}^T\mathbf{B}_1^T\mathbf{P}_2\mathbf{w} - \lambda_2\mathbf{v}^T\mathbf{v}. \end{aligned} \tag{39}$$

Let

$$\begin{aligned} \zeta_2 &= \begin{bmatrix} \mathbf{x} \\ \mathbf{v} \\ \mathbf{w} \end{bmatrix}, \\ \chi_2 &= \begin{bmatrix} \mathbf{P}_2\overline{\mathbf{A}} + \overline{\mathbf{A}}^T\mathbf{P}_2 + \lambda_2\mathbf{W}_1^T\mathbf{W}_1 + \overline{\mathbf{C}}_2^T\overline{\mathbf{C}}_2 & \mathbf{P}_2\mathbf{F}_1 & \mathbf{P}_2\mathbf{B}_1 \\ * & -\lambda_2 I & 0 \\ * & * & -\gamma I \end{bmatrix}, \end{aligned} \tag{40}$$

and if $\chi_2 < 0$, then we have

$$\mathbf{J}_z = \int_0^\infty \left(\mathbf{z}^T\mathbf{z} - \gamma\mathbf{w}^T\mathbf{w} \right) \mathrm{d}t \leq \int_0^\infty \zeta_2^T \chi_2 \zeta_2 \mathrm{d}t < 0. \tag{41}$$

It is equivalent to

$$\|\mathbf{z}\| < \gamma \|\mathbf{w}\|. \tag{42}$$

Similarly, it is equivalent to obtain $\chi_1 < 0$ through $\chi_2 < 0$ by using Schur complement, and $\chi_2 < 0$ can ensure being $\dot{\mathbf{V}}_2 < 0$, which implies that system (31) is asymptotically stable. For $\forall \mathbf{w} \in L_2[0, +\infty)$, one can get $\mathbf{J}_z < 0$ from $\dot{\mathbf{V}}_2 < 0$, that is, $\|\mathbf{z}\| < \gamma\|\mathbf{w}\|$ (see (41) and (42)). Furthermore, system (31) has H_∞ performance β if and only if the controlled system is asymptotically stable and the inequality $\|\mathbf{z}\| < \gamma\|\mathbf{w}\|$ holds for $\forall \widetilde{\mathbf{w}} \in L_2[0, +\infty)$ under $\chi_2 < 0$ conditions.

The proof is completed.

To guarantee the solvability of (34) in *Theorem* 3, *Theorem* 4 is presented herein. □

Theorem 4. *For given positive scalars γ and λ_2, the closed-loop system (31) is asymptotically stable and has a prescribed H_∞ disturbance attenuation level $\gamma > 0$, if there exist symmetric positive definite matrix $\mathbf{Q}$, $\mathbf{R}$ with appropriate dimension and the gain matrix $\mathbf{K}$ such that the following inequality holds:*

$$\begin{bmatrix} \mathbf{A}\mathbf{Q} + \mathbf{B}_2 + \mathbf{Q}\mathbf{A}^T + \mathbf{R}^T\mathbf{B}_2^T & \mathbf{F}_1 & \mathbf{B}_1 & \lambda_2\mathbf{Q}\mathbf{W}_1^T & \mathbf{Q}\mathbf{C}_2^T + \mathbf{R}^T\mathbf{D}_2^T \\ * & -\lambda_2\mathbf{I} & 0 & 0 & 0 \\ * & * & -\gamma\mathbf{I} & 0 & 0 \\ * & * & * & -\mathbf{I} & 0 \\ * & * & * & * & -\mathbf{I} \end{bmatrix} < 0, \tag{43}$$

where $\mathbf{K} = \mathbf{R}\mathbf{Q}^{-1}$.

Proof. The term $\chi_2 < 0$ is left multiplied by diag $\{\mathbf{P}_2^{-1}, \mathbf{I}, \mathbf{I}, \mathbf{I}, \mathbf{I}\}$ and right multiplied by diag $\{\mathbf{P}_2^{-1}, \mathbf{I}, \mathbf{I}, \mathbf{I}, \mathbf{I}\}$; apply Schur complement and let $Q = \mathbf{P}_2^{-1}$ and $R = KQ$; by further derivations, we can obtain (43). The proof is completed. □

4.2. Design Procedure of the Proposed HFTC Scheme. With the aforementioned Theorem 1 to Theorem 4, the actuator fault occurring at the ASS can be estimated with the designed robust H_∞ observer, and then a hybrid fault-tolerant controller is further developed; the detailed design procedure is formulated as follows:

Step 1. Solve *Theorem 2* so as to get L from (29) and estimate the actuator faults by using $\widehat{\mathbf{f}} = \mathbf{C}_{\mathrm{ef}}\widehat{\bar{\mathbf{x}}}$ in (10).

Step 2. Construct compensation controller as $u_c = -M\mathbf{C}_{\mathrm{ef}}\widehat{\bar{\mathbf{x}}} = -M\widehat{f}$.

Step 3. Solve *Theorem 4* to obtain $\mathbf{K} = \mathbf{R}\mathbf{Q}^{-1}$, that is, $\mathbf{u}_n = Kx_f$, and then the proposed HFTC in (30) is achieved and the corresponding control block is shown in Figure 2.

From Figure 2, it is obvious that the proposed hybrid fault-tolerant controller is composed of a nominal state-feedback controller and a robust H_∞ observer. The former one only works under the fault-free condition, and the latter one can accurately estimate the actuator faults, and the designed fault-tolerant controller can be realized by combing the nominal state-feedback controller and the robust H_∞ output-feedback observer under the actuator fault condition.

5. Simulation Investigation and Discussion

In this section, to verify the effectiveness and advantages of the proposed HFTC, the performance analysis and comparative simulations are conducted for the following three types of vehicle ASSs described as follows:

(i) NSFC-without fault: only the nominal state-feedback controller works under the actuator fault-free condition.

(ii) NSFC-with fault: only the nominal state-feedback controller works under the actuator fault condition.

(iii) HFTC-with fault: the designed hybrid fault-tolerant controller works under the actuator fault condition.

Besides, the controller gain is calculated through MATLAB 2016a® LMI toolbox and FEASP Solver (MathWorks, Inc., Natick, MA, USA), and the simulation is conducted under MATLAB 2016a® Simulink (MathWorks, Inc., Natick, MA, USA). The half-vehicle model parameters are listed in Table 1 [37].

5.1. Performance Analysis under the General Actuator Fault. The random road disturbance is assumed as a vibration signal that is consistent and typically specified as a white noise expressed by [38]

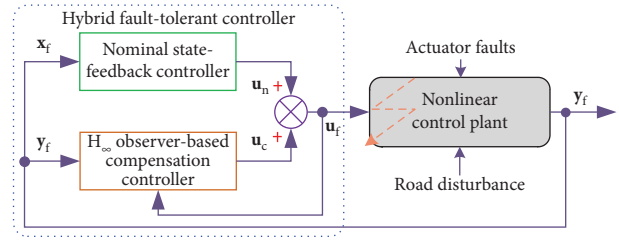

Figure 2: Control block of the designed hybrid fault-tolerant controller.

Table 1: Parameters of half-vehicle suspension.

Parameter	Value
m_s/kg	1235
$m_{uf}(m_{ur})$/kg	49
I_y/(kg·m^2)	1731
$k_f(k_r)$/(N·m^{-1})	22,741
k_{tf}/(N·m^{-1})	492,982
k_{tr}/(N·m^{-1})	302,342
c_f/(N·s·m^{-1})	1221
c_r/(N·s·m^{-1})	1228
a/m	1.2
b/m	1.5

$$\dot{z}_r = -2\pi f_0 z_r + 2\pi n_0 \omega \sqrt{G_q(n_0)v}, \tag{44}$$

where $G_q(n_0)$ is selected as $1024 \times 10^{-6}\,\mathrm{m}^3$, $v = 20$ m/s, the lower cutoff frequency of road profile $f_0 = 0.1$, the reference spatial frequency $n_0 = 0.1$ (1/m), and $\omega(t)$ is zero mean white Gaussian noise with identity power spectral density with the sample time of 0.01s.

The fault signal and its corresponding fault estimation are revealed in Figure 3(a), and the fault estimation error is displayed in Figure 3(b), respectively. Note that the estimation error of the actuator fault is calculated by $\Delta f = f - \widehat{f}$.

It is observed from Figure 3 that the estimation error of the actuator fault has a peak value less than ±0.05, implying that the designed H_∞ observer can accurately estimate the actuator fault. Besides, Figure 4 is presented to show the performance comparisons of $\ddot{z}_c$, $\ddot{\phi}$, Δy_f and Δy_r, and F_{tf} and F_{tr} for the three types of ASSs in time domain.

Additionally, it can be concluded from Figure 4(a) that the response of $\ddot{z}_c$ becomes obviously deteriorated in case of the NSFC-without fault, yet $\ddot{z}_c$ of the HFTC-with fault can yield better ride comfort performance in comparisons with the NSFC-with fault, while the responses of $\ddot{\phi}$ in Figure 4(b) remain basically unchanged for these three ASSs. Moreover, it can be inferred from Figures 4(c) to 4(f) that Δy_f and Δy_r and F_{tf} and F_{tr} are effectively reduced for the faulty ASS in case of the proposed HFTC-with fault, which can prevent suspension breakdown when suspension deflection is out of its limitation and can further improve tire life span and vehicle handling stability simultaneously.

Moreover, Figure 5 plots the control forces of the front and rear actuators with the designed HFTC. It is seen from

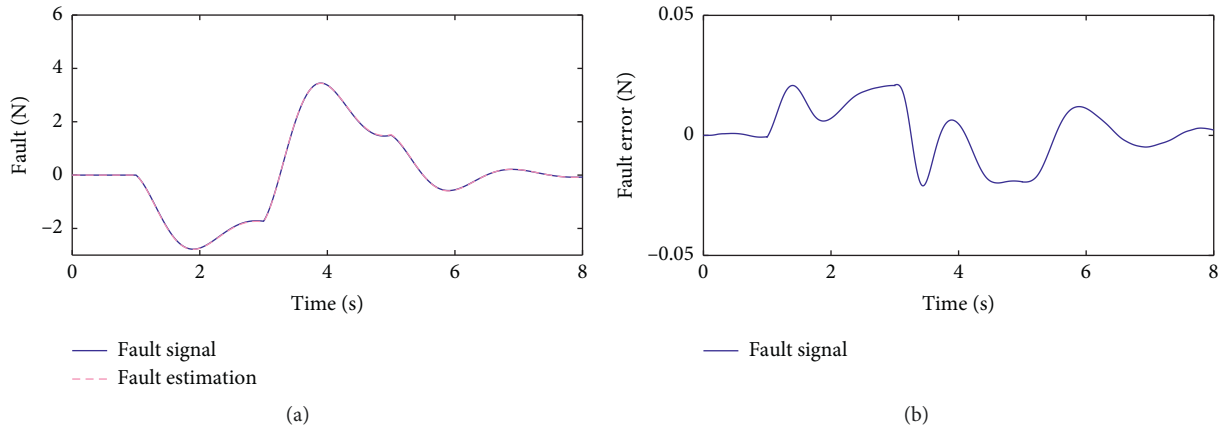

Figure 3: The variations of (a) fault estimation and (b) fault estimation error for the general fault signal.

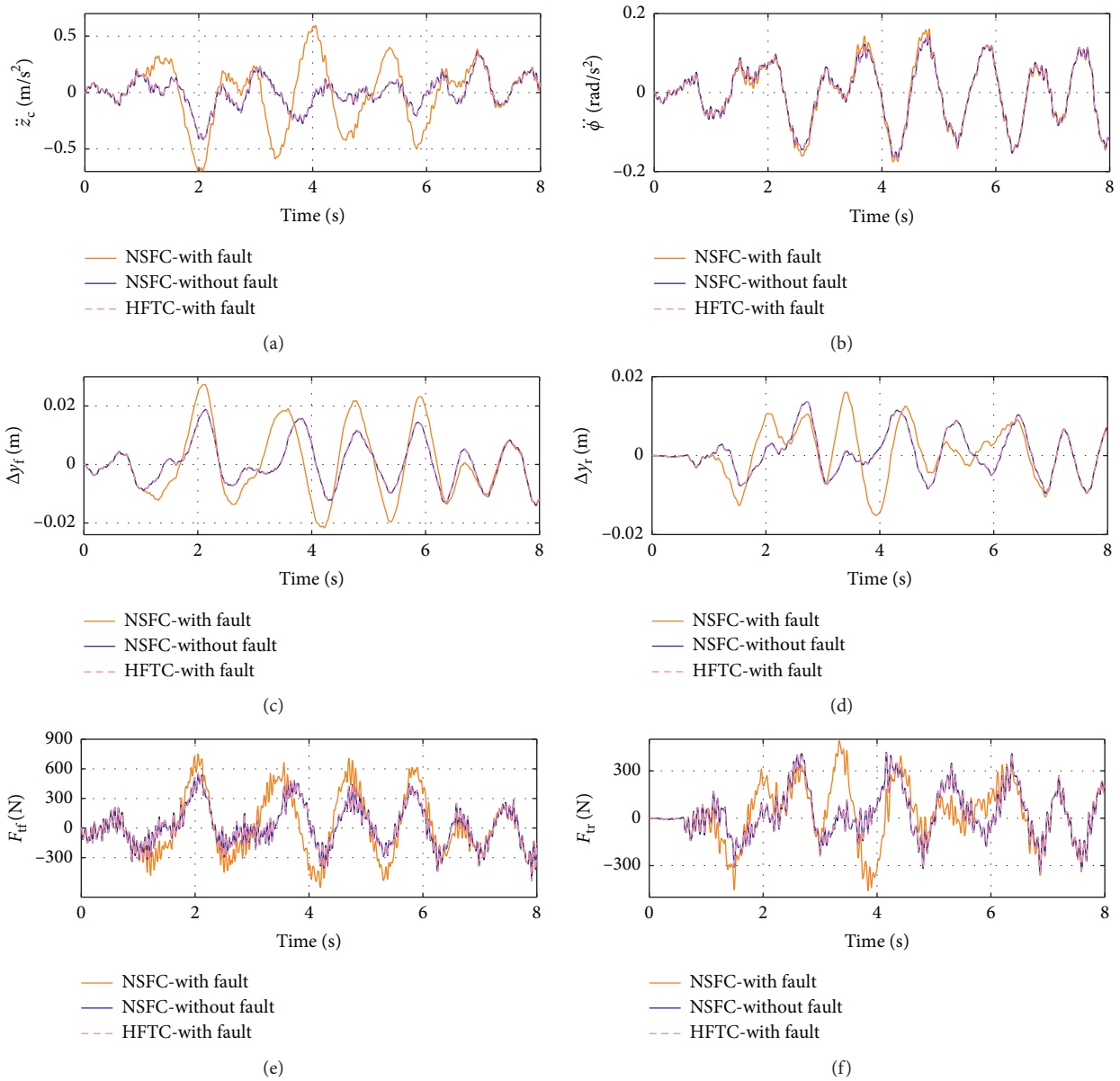

Figure 4: The response comparisons of ASS with the general fault signal under random road disturbance.

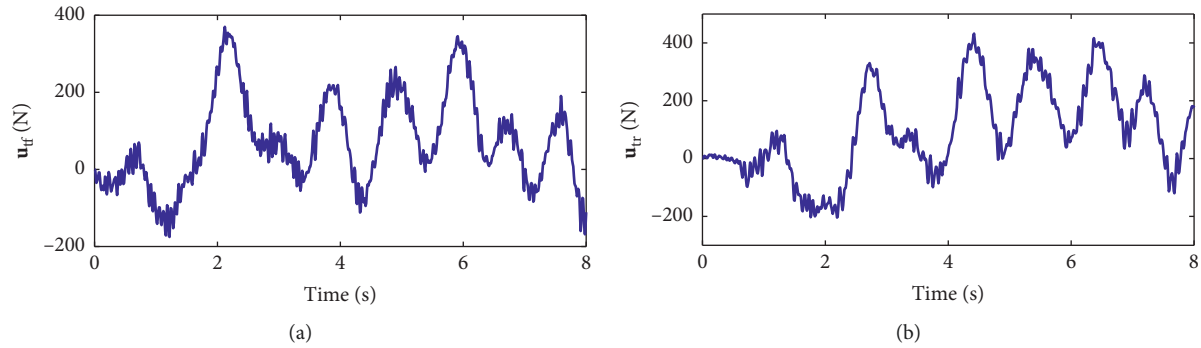

Figure 5: The control forces of (a) the front actuator and (b) rear actuator under the random road disturbance.

Figure 5 that the control forces vary with the change of fault signals on time, which illustrates that the proposed HFTC can generate the compensative control forces to reduce the negative effects of the actuator fault on the closed-loop system.

5.2. Performance Analysis under the Sinusoidal Actuator Fault. To further evaluate the proposed HFTC, the sinusoidal signal is used to mimic the actuator faults and validate the effectiveness of the proposed HFTC. Figure 6 shows the variations of the front actuator fault and the corresponding estimation as well as the fault estimation error. It is easily found that the designed robust H_∞ observer can accurately estimate the actuator fault with the fault estimation error of −0.02 N to 0.02 N.

Figure 7 shows the response comparisons of $\ddot{z}_c$ and $\ddot{\phi}$, Δy_f and Δy_r, and F_{tf} and F_{tr} for the three types of ASSs under the random road disturbance, respectively. It is observed that $\ddot{z}_c$ of the HFTC-with fault is significantly improved as compared with the NSFC-without fault, while $\ddot{\phi}$ stays the same in case of these three ASSs. Additionally, the safety constraint performance indicators of Δy_f and Δy_r and F_{tf} and F_{tr} for the ASS become deteriorated in case of the NSFC-without fault. However, these four performance indicators can remain stable for the faulty ASS with the proposed HFTC.

Figure 8 shows the variations of control forces at the front and rear actuator, which illustrates that our proposed HFTC can produce the desirable control forces to compensate for the performance penalties of the ASS in the presence of the sinusoidal actuator fault.

Additionally, in order to make a comprehensive performance comparisons of the faulty ASS with these three control schemes, Table 2 summarizes the root-mean-square (RMS) values of $\ddot{z}_c$, $\ddot{\phi}$, Δy_f, Δy_r, F_{tf}, and F_{tr} under the sinusoidal fault signal. It is concluded from Table 2 that compared to the NSFC-without fault, the performance indicators of $\ddot{z}_c$, $\ddot{\phi}$, Δy_f and Δy_r, and F_{tf} and F_{tr} are, respectively, increased about 61.8%, 3.20%, 26.6%, 69.2%, 16.7%, and 63.3% in case of the NSFC-with fault. However, all the performance indicators for the ASS with the proposed HFTC can remain basically unchanged as compared with the NSFC-with fault.

5.3. Comparative Investigation. To demonstrate the differences between the proposed HFTC and the most related FTC approach in [32], the comparison investigation is performed. Herein, the bump road is used as the road disturbance, which is expressed by [7]

$$z_r = \begin{cases} \dfrac{A_m}{2}\left(1 - \cos\dfrac{2\pi u}{L}t\right), & 0 \le t \le \dfrac{L}{u}, \\ 0, & t > \dfrac{L}{u}, \end{cases} \tag{45}$$

where A_m, L, and u represent the height and length of bump road and vehicle forward speed, respectively. Note that their corresponding values are extracted from [7] as $A_m = 100$ (mm), $L = 5$ m, and $u = 45$ (km/h).

In [31], a proportional-integral observer (PIO) was used to estimate the actuator fault in the active suspension system, which is different from our proposed robust H_∞ observer (RHO). To reveal the differences for the PIO and RHO, the fault estimation and the corresponding fault estimation errors are presented in Figure 9. It can be obtained from Figure 9 that our designed RHO has higher estimation accuracy as compared with the PIO in [31]. However, only the design approach of the PIO is included in [31] for the suspension system, while the fault-tolerant controller design is not included.

Moreover, in [32], both the PIO and the corresponding fault-tolerant controller were addressed, so it is very suitable to conduct the comparative studies on the proposed HFTC and the fault-tolerant controller (FTC) in [32] for the ASS. The response comparisons of the simulation results are shown in Figure 10. It can be observed that $\ddot{z}_c$ of the HFTC-with fault is improved in comparison with the FTC in [32]. However, the pitch angular acceleration $\ddot{\phi}$ stays nearly the same for the proposed HFTC and the FTC in [32].

Besides, we can conclude that the tire dynamic loads of F_{tf} and F_{tr} are reduced by using the proposed HFTC approach, which can prevent suspension breakdown and simultaneously improve the tire life span and vehicle handling stability when encountering a certain actuator fault. Overall, the proposed HFTC has better control performances.

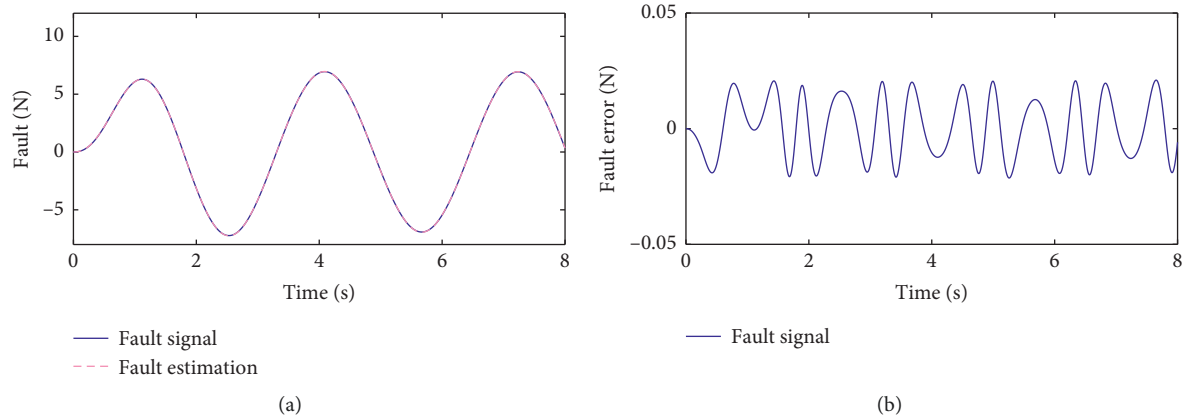

Figure 6: The variations of (a) fault estimation and (b) fault estimation error for the sinusoidal fault signal.

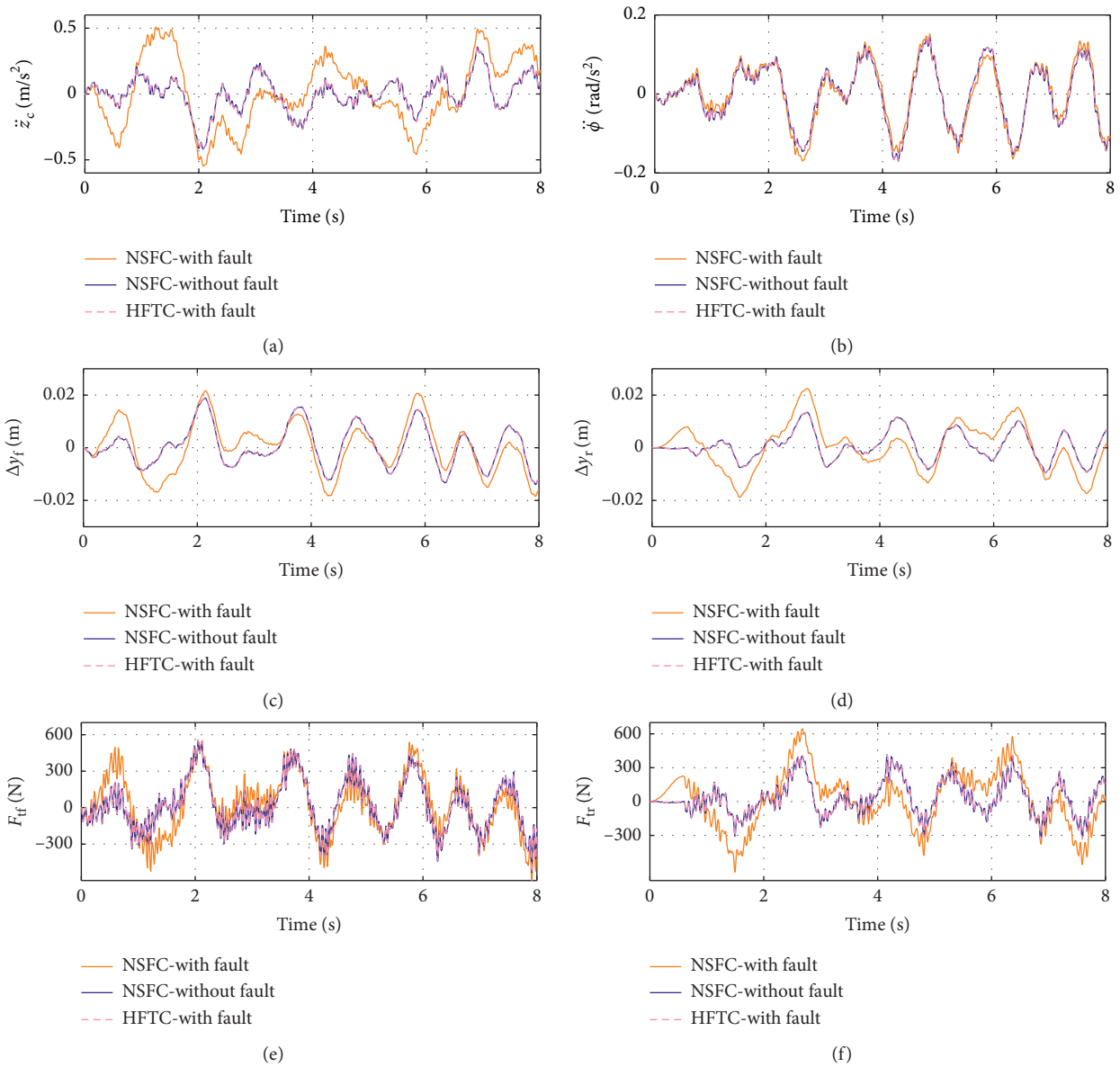

Figure 7: The response comparisons of ASS with the sinusoidal fault signal under the random road disturbance.

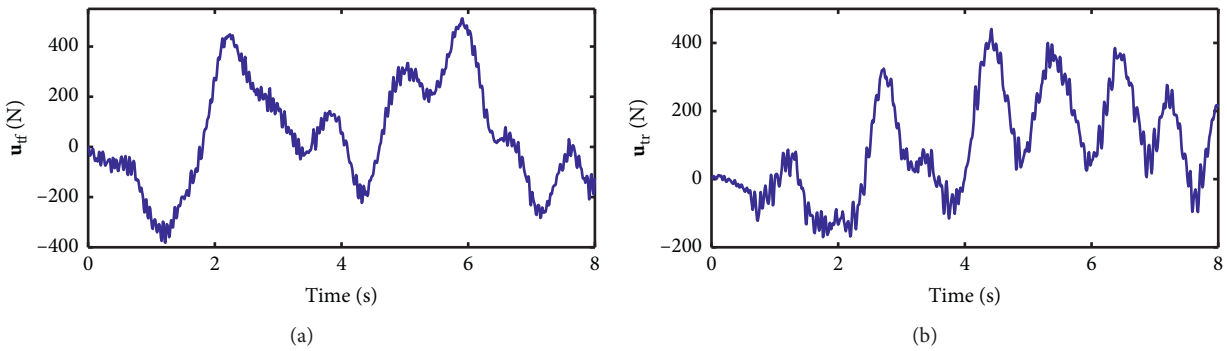

Figure 8: The control forces of (a) the front actuator and (b) rear actuator under the random road disturbance.

Table 2: The comparisons of RMS values under the random road disturbance.

	NSFC-without fault	NSFC-with fault	HFTC-with fault
$\ddot{z}_c/(m/s^2)$	0.1293 (—)	0.2577 (↑61.8%)	0.1293
$\ddot{\phi}/(rad/s^2)$	0.1853 (—)	0.1913 (↑3.20%)	0.1853
$\Delta y_f/m$	0.0075 (—)	0.0950 (↑26.6%)	0.0075
$\Delta y_r/m$	0.0052 (—)	0.0880 (↑69.2%)	0.0052
F_{tf}/N	202.1314 (—)	237.7155 (↑16.7%)	203.8815
F_{tr}/N	150.4045 (—)	245.5683 (↑63.3%)	150.1407

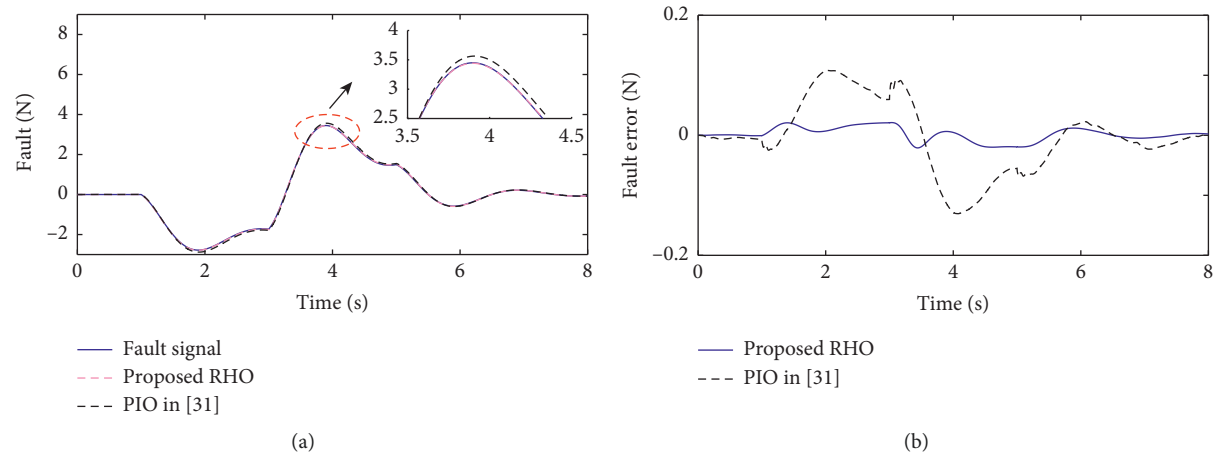

Figure 9: The comparison of (a) fault estimation and (b) fault estimation error.

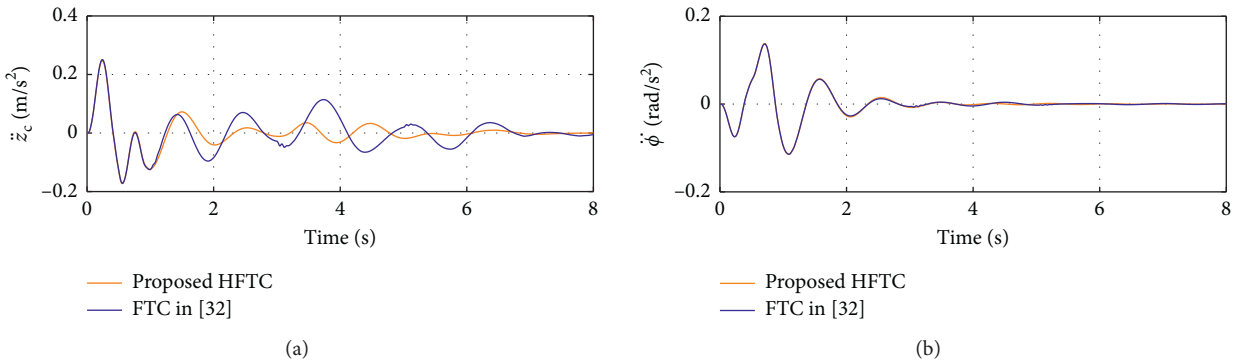

Figure 10: Continued.

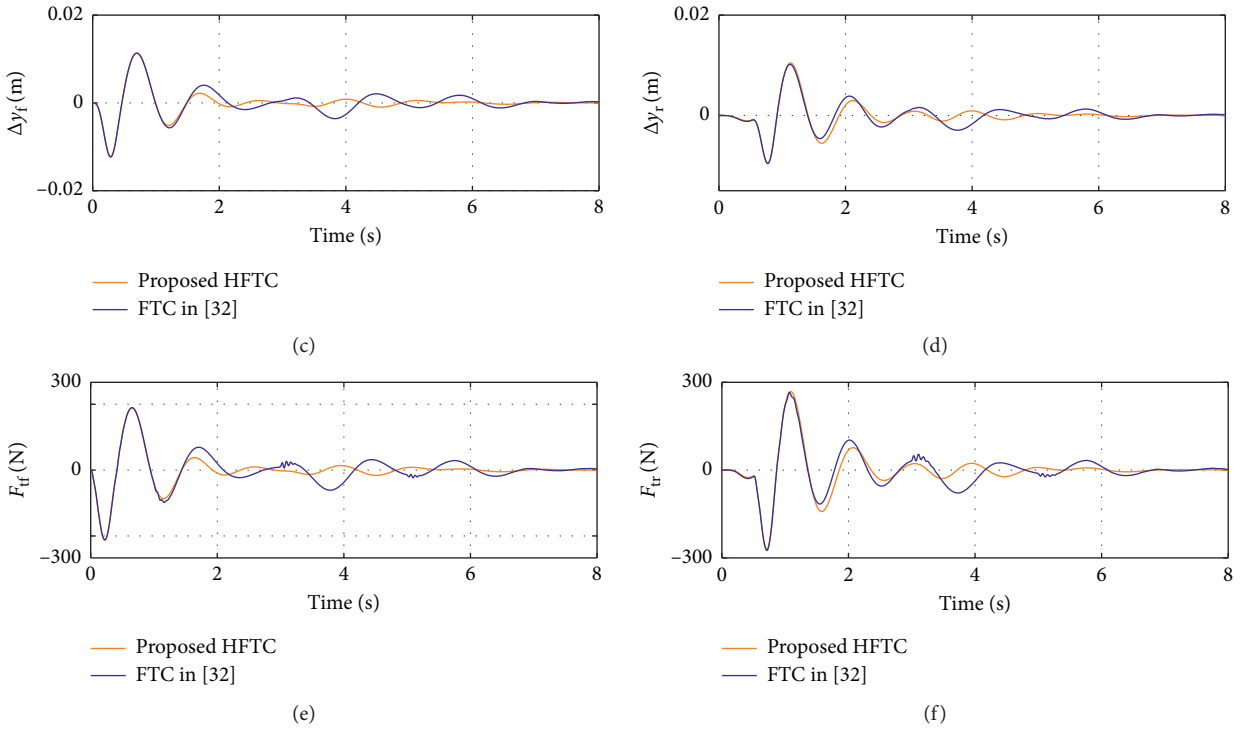

Figure 10: The response comparisons of the ASS with random fault signal under bump road disturbance.

6. Conclusions

This paper has presented a hybrid fault-tolerant controller design for a class of nonlinear ASSs in the presence of the actuator faults and road disturbances. With the help of system augmentation technique, we established the augmented closed-loop system model of faulty ASS. Based on this model, we further proposed the hybrid fault-tolerant controller consisting of a nominal state-feedback controller and a robust H_∞ observer, which can not only achieve the asymptotic stability of this ASS under fault-free condition but also reduce the negative effects resulting from the unknown actuator faults and road disturbances under the fault condition. In addition, the designed hybrid fault-tolerant controller has been validated to be effective and feasible by using the more convincing numerical simulation results. Future work will focus on the controller design and verification for a repetitive control system [39, 40] with multimode actuator faults; meanwhile, the actuator input delay and saturation constraint will be considered in the corresponding fault-tolerant controller design.

Nomenclature

m_s: Mass of vehicle body
I_y: Rotary inertia of vehicle body
ϕ: Pitch angular displacement
$\ddot{\phi}$: Pitch angular acceleration
m_{uf}: Sprung mass of front suspension
m_{ur}: Unsprung mass of rear suspension
c_f: Damping coefficient of front suspension
c_r: Damping coefficient of rear suspension
k_f: Stiffness coefficient of front suspension
k_r: Stiffness coefficient of rear suspension
k_{tf}: Stiffness coefficient of front tire wheel
k_{tf}: Stiffness coefficient of rear tire wheel
a: Distance from CG to the front suspension
b: Distance from CG to the rear suspension
v: Vehicle forward speed
z_c: Vertical displacement of vehicle body
$\ddot{z}_c$: Vertical acceleration of vehicle body
z_{sf}: Sprung-mass displacement of the front wheel
z_{sr}: Sprung-mass displacement of the rear wheel
z_{uf}: Unsprung-mass displacement of the front wheel
z_{ur}: Unsprung-mass displacement of the rear wheel
z_{rf}: Road disturbance of the front wheel
z_{rr}: Road disturbance of the rear wheel
u_f: Control force of the front actuator with input delay
u_r: Control force of the rear actuator with input delay
$\mathbf{I}_2$: Identity matrix with 2×2 order
CG: Center of gravity $i = f, r$ for front and rear wheel.

Data Availability

The data used to support the findings of this study are available from the corresponding author upon request.

Conflicts of Interest

The authors declare that they have no potential conflicts of interest that could have appeared to influence the work reported in this paper.

Acknowledgments

This work was supported by the National Natural Science Foundation of China under grant nos. 51675423 and 51305342 and Primary Research & Development Plan of Shaanxi Province under grant no. 2017GY-029.

References

[1] A. S. Yıldız, S. Sivrioğlu, E. Zergeroğlu, and Ş. Çetin, "Nonlinear adaptive control of semi-active MR damper suspension with uncertainties in model parameters," *Nonlinear Dynamics*, vol. 79, no. 4, pp. 2753–2766, 2015.

[2] S. M. Savaresi and C. Spelta, "A single-sensor control strategy for semi-active suspensions," *IEEE Transactions on Control Systems Technology*, vol. 17, no. 1, pp. 143–152, 2009.

[3] M. Zapateiro, F. Pozo, H. R. Karimi, and N. Luo, "Semiactive control methodologies for suspension control with magnetorheological dampers," *IEEE/ASME Transactions on Mechatronics*, vol. 17, no. 2, pp. 370–380, 2012.

[4] V. Sankaranarayanan, M. E. Emekli, B. A. Gilvenc et al., "Semiactive suspension control of a light commercial vehicle," *IEEE/ASME Transactions on Mechatronics*, vol. 13, no. 5, pp. 598–604, 2008.

[5] S. M. Savaresi, C. Poussot-Vassal, C. Spelta, O. Sename, and L. Dugard, *Semi-Active Suspension Control Design for Vehicles*, Elsevier, Amsterdam, Netherlands, 2010.

[6] L.-X. Guo and L.-P. Zhang, "Robust H_∞ control of active vehicle suspension under non-stationary running," *Journal of Sound and Vibration*, vol. 331, no. 26, pp. 5824–5837, 2012.

[7] W. Sun, H. Pan, Y. Zhang, and H. Gao, "Multi-objective control for uncertain nonlinear active suspension systems," *Mechatronics*, vol. 24, no. 4, pp. 318–327, 2014.

[8] H. Pang, Y. Chen, J. Chen, and X. Liu, "Design of LQG controller for active suspension without considering road input signals," *Shock and Vibration*, vol. 2017, Article ID 6573567, 13 pages, 2017.

[9] R.-J. Lian, "Enhanced adaptive self-organizing fuzzy sliding-mode controller for active suspension systems," *IEEE Transactions on Industrial Electronics*, vol. 60, no. 3, pp. 958–968, 2013.

[10] X.-M. Zhang and Q.-L. Han, "Event-triggered H_∞ control for a class of nonlinear networked control systems using novel integral inequalities," *International Journal of Robust and Nonlinear Control*, vol. 27, no. 4, pp. 679–700, 2017.

[11] L. Zhou, J. She, and S. Zhou, "Robust H_∞ control of an observer-based repetitive-control system," *Journal of the Franklin Institute*, vol. 355, no. 12, pp. 4952–4969, 2018.

[12] V. S. Deshpande, B. Mohan, P. D. Shendge, and S. B. Phadke, "Disturbance observer based sliding mode control of active suspension systems," *Journal of Sound and Vibration*, vol. 333, no. 11, pp. 2281–2296, 2014.

[13] H. Pang, J. N. Chen, and K. Liu, "Adaptive backstepping tracking control for vehicle semi-active suspension system with magnetorheological damper," *Acta Armamentarii*, vol. 7, no. 23, 2017.

[14] W. Sun, H. Gao, and O. Kaynak, "Adaptive backstepping control for active suspension systems with hard constraints," *IEEE/ASME Transactions on Mechatronics*, vol. 18, no. 3, pp. 1072–1079, 2013.

[15] H. Du, N. Zhang, P. O. Sydney, and N. S. Broadway, "Takagi-Sugeno fuzzy control scheme for electrohydraulic active suspensions," *Control and Cybernetics*, vol. 39, no. 4, pp. 1095–1115, 2010.

[16] H. Li, J. Yu, C. Hilton, and H. Liu, "Adaptive sliding-mode control for nonlinear active suspension vehicle systems using T-S fuzzy approach," *IEEE Transactions on Industrial Electronics*, vol. 60, no. 8, pp. 3328–3338, 2013.

[17] M. Moradi and A. Fekih, "A stability guaranteed robust fault tolerant control design for vehicle suspension systems subject to actuator faults and disturbances," *IEEE Transactions on Control Systems Technology*, vol. 23, no. 3, pp. 1164–1171, 2015.

[18] M. Moradi and A. Fekih, "Adaptive PID-sliding-mode fault-tolerant control approach for vehicle suspension systems subject to actuator faults," *IEEE Transactions on Vehicular Technology*, vol. 63, no. 3, pp. 1041–1054, 2014.

[19] R. Wang, H. Jing, H. R. Karimi, and N. Chen, "Robust fault-tolerant H_∞ control of active suspension systems with finite-frequency constraint," *Mechanical Systems and Signal Processing*, vol. 62-63, pp. 341–355, 2015.

[20] H. Jing, R. Wang, H. R. Karimi, M. Chadli, C. Hu, and F. Yan, "Robust output-feedback based fault-tolerant control of active suspension with finite-frequency constraint," *IFAC-PapersOnLine*, vol. 48, no. 21, pp. 1173–1179, 2015.

[21] B. Liu, M. Saif, and H. Fan, "Adaptive fault tolerant control of a half-car active suspension systems subject to random actuator failures," *IEEE/ASME Transactions on Mechatronics*, vol. 21, no. 6, pp. 2847–2857, 2016.

[22] S. Liu, H. Zhou, X. Luo, and J. Xiao, "Adaptive sliding fault tolerant control for nonlinear uncertain active suspension systems," *Journal of the Franklin Institute*, vol. 353, no. 1, pp. 180–199, 2016.

[23] T. Alizadeh and S. Barzegari, "Fault-tolerant control of electromagnetic suspension system with simultaneous sensor and actuator faults," in *Proceedings of the IEEE Asian Control Conference*, Kota Kinabalu, Malaysia, May 2015.

[24] Y. Song and X. Yuan, "Low-cost adaptive fault-tolerant approach for semiactive suspension control of high-speed trains," *IEEE Transactions on Industrial Electronics*, vol. 63, no. 11, pp. 7084–7093, 2016.

[25] M. Q. Nguyen, O. Sename, and L. Dugard, "An LPV fault tolerant control for semi-active suspension-scheduled by fault estimation," *IFAC-PapersOnLine*, vol. 48, no. 21, pp. 42–47, 2015.

[26] H. Li, H. Liu, H. Gao, and P. Shi, "Reliable fuzzy control for active suspension systems with actuator delay and fault," *IEEE Transactions on Fuzzy Systems*, vol. 20, no. 2, pp. 342–357, 2012.

[27] H. Li, H. Gao, H. Liu, and M. Liu, "Fault-tolerant H_∞ control for active suspension vehicle systems with actuator faults," *Proceedings of the Institution of Mechanical Engineers, Part I: Journal of Systems and Control Engineering*, vol. 226, no. 3, pp. 348–363, 2012.

[28] W. Sun, H. Gao, H. Pan, and J. Yu, "Reliability control for uncertain half-car active suspension systems with possible actuator faults," *IET Control Theory & Applications*, vol. 8, no. 9, pp. 746–754, 2014.

[29] J. Qiu, M. Ren, Y. Guo, and Y. Zhao, "Active fault-tolerant control for vehicle active suspension systems in finite-frequency domain," *IET Control Theory & Applications*, vol. 5, no. 13, pp. 1544–1550, 2011.

[30] H. Pan, H. Li, W. Sun, and Z. Wang, "Adaptive fault-tolerant compensation control and its application to nonlinear suspension systems," *IEEE Transactions on Systems, Man, and Cybernetics: Systems*, vol. 99, pp. 1–11, 2018.

[31] M.-H. Do, D. Koenig, and D. Theilliol, "Robust H_∞ proportional-integral observer for fault diagnosis: application to

vehicle suspension," *IFAC-PapersOnLine*, vol. 51, no. 24, pp. 536–543, 2018.

[32] S. Aouaouda, T. Bouarar, and O. Bouhali, "Fault tolerant tracking control using unmeasurable premise variables for vehicle dynamics subject to time varying faults," *Journal of the Franklin Institute*, vol. 351, no. 9, pp. 4514–4537, 2014.

[33] S. Yin, H. Yang, and O. Kaynak, "Sliding mode observer-based FTC for Markovian jump systems with actuator and sensor faults," *IEEE Transactions on Automatic Control*, vol. 62, no. 7, pp. 3551–3558, 2017.

[34] Z. Ping and J. Huang, "Global robust output regulation for a class of multivariable systems," *International Journal of Robust and Nonlinear Control*, vol. 23, no. 3, pp. 241–261, 2013.

[35] Z. Chen, L. Liu, and J. Huang, "Global tracking and disturbance rejection of a class of lower triangular systems subject to an unknown exosystem," in *Proceedings of the IEEE International Conference on Control & Automation*, IEEE, Xiamen, China, December 2010.

[36] R. A. Horn and F. Zhang, *The Schur Complement and its Applications*, Springer, New York, NY, USA, 2005.

[37] S. W. Yu, *Matlab Vehicle Engineering Application*, Tsinghua University Press, Beijing, China, 2014.

[38] H. Pang, W.-Q. Fu, and K. Liu, "Stability analysis and fuzzy smith compensation control for semi-active suspension systems with time delay," *Journal of Intelligent & Fuzzy Systems*, vol. 29, no. 6, pp. 2513–2525, 2015.

[39] L. Zhou, J. H. She, S. W. Zhou et al., "Compensation for state-dependent nonlinearity in a modified repetitive control system," *International Journal of Robust and Nonlinear Control*, vol. 28, no. 1, pp. 213–226.

[40] L. Zhou, J. H. She, X. M. Zhang et al., "Performance enhancement of repetitive-control systems and application to tracking control of chuck-workpiece systems," *IEEE Transactions on Industrial Electronics*, p. 1, 2019.